ChemComm

COMMUNICATION

View Article Online
View Journal | View Issue

Cite this: *Chem. Commun.*, 2018, **54**, 4878

Received 1st March 2018,
Accepted 3rd April 2018

DOI: 10.1039/c8cc01715h

rsc.li/chemcomm

A caged metabolic precursor for DT-diaphorase-responsive cell labeling†

Ruibo Wang,[a] Kaimin Cai,[a] Hua Wang,[a] Chen Yin[b] and Jianjun Cheng *[acdefg]

In this study, we report incorporation of a covalent linker at the anomeric position of *N*-azidoacetylmannosamine (ManNAz) for caging its metabolic process. We synthesized a DT-diaphorase-responsive metabolic precursor, HQ-NN-AAM, using an optimized linker. The caged metabolite showed responsiveness to DT-diaphorase *in vitro*, resulting in metabolic incorporation of an azido sugar into the cell surface in multiple cell lines.

The research on metabolic glycoengineering has evolved rapidly over the last few decades; metabolic glycoengineering utilizes endogenous enzymes to process unnatural glycan substrates and introduces chemical functional groups into proteoglycans and glycoproteins.[1–3] Based on bioorthogonal Click chemistry,[4,5] these chemical anchors serve as powerful tools to understand and study glycans both on cell surfaces and in the cytoplasm, which result in improved understanding about proteomics,[6–8] cell–cell interaction,[9] and cell metastasis.[10] Metabolic incorporation of an unnatural sugar has opened up new directions in applied science, especially in drug delivery and tumor imaging.[11–15] One of the most studied unnatural sugars, *N*-azidoacetylmannosamine (ManNAz), shares the same metabolic process with *N*-acetylmannosamine.[6] The native hexose undergoes several steps of enzymatic processing and yields cytidine monophosphate-sialic acid (CMP-Neu5Ac), which is conjugated to cell surface glycans through post-translational modification in the Golgi apparatus.[3] This metabolic process is shared by most mammalian cell types; thus, the use of ManNAz to selectively label specific types of cells has been proven to be difficult without interfering with their cellular metabolic machinery.[3]

At present, there are a few studies on controlling the metabolic labelling of ManNAz through different strategies. Cellular uptake levels determine the amount of potential unnatural sugars that can be metabolized in specific cells. Thus, researchers have developed delivery methods to enhance the cellular uptake[16,17] or spatial availability of ManNAz towards the cells of interest.[13] Since ManNAz needs to go through metabolic processes inside cells, its modification with caging groups at different positions, namely anomeric[14] or C-6 hydroxy groups,[18,19] of the unnatural hexose would provide extra control on its metabolic process. The metabolic precursor usually consists of three components: a metabolic labeling agent, a self-immolative linker, and a trigger-cleavable cage group.[20] These metabolic precursors have been demonstrated to have great potential in cancer imaging[19] and targeted delivery of drugs.[14] However, in some cases, the self-immolative linker exhibits compromised stability under physiological conditions; this results in the cleavage of the caged group even when the respective trigger enzyme is absent.[18,19] For example, it has been reported that a caged precursor with a peptide conjugated to Ac_3ManNAz through a carbonate bond at the C-6 position shows nonenzymatic carbonate hydrolysis in the absence of the trigger enzyme in degradation studies.[18] Clearly, it is challenging to achieve trigger-specific metabolic labeling with these existing linkers that can be cleaved nonspecifically in a cellular environment. Our group has previously developed a selective labeling technique, which demonstrates that ether linkages at the anomeric position of ManNAz successfully control the labeling process of ManNAz,[14] and selective metabolic labeling of cancer cells based on their different enzymatic activities is achieved. However, the anomeric ether bond formation requires strong acidic conditions, which hinder the incorporation of acid-labile caging groups such as Boc-protected oligopeptides. Therefore, it is important to design metabolic precursors with controlled decaging processes

[a] *Department of Materials Science and Engineering, University of Illinois at Urbana-Champaign, Urbana, IL 61801, USA. E-mail: Jianjunc@illinois.edu*
[b] *Department of Chemistry, Tsinghua University, Beijing, 100084, China*
[c] *Frederick Seitz Materials Research Laboratory, University of Illinois at Urbana–Champaign, Urbana, IL 61801, USA*
[d] *Department of Bioengineering, University of Illinois at Urbana–Champaign, Urbana, IL 61801, USA*
[e] *Beckman Institute for Advanced Science and Technology, University of Illinois at Urbana–Champaign, Urbana, IL 61801, USA*
[f] *Department of Chemistry, University of Illinois at Urbana–Champaign, Urbana, IL 61801, USA*
[g] *Carl R. Woese Institute for Genomic Biology, University of Illinois at Urbana–Champaign, Urbana, IL 61801, USA*

† Electronic supplementary information (ESI) available. See DOI: 10.1039/c8cc01715h

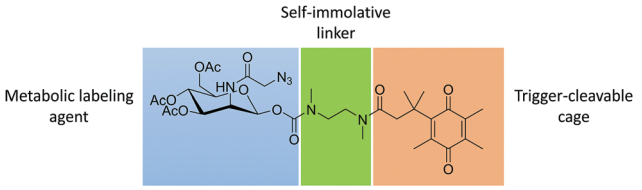

Scheme 1 Schematic of the three components of the caged metabolite HQ-NN-AAM.

and feasibility to incorporate a wide range of trigger-responsive functionalities.

Herein, we report a new metabolic precursor (Scheme 1), HQ-NN-AAM, which contains a DT-diaphorase (DTD)-responsive trimethyl quinone moiety (HQ)[21,22] and a self-immolative dimethylethylenediamine (NN) linker attached at the anomeric position of ManNAz through a *N*-methyl carbamate linkage.[23,24] The linkage was selected based on our study on the unspecific cleavage of various common linkers in typical cellular environments. The self-immolative linker also enables a mild synthetic condition and avoids harsh acidic glycosylation reactions to couple trigger groups at the anomeric position. HQ-NN-AAM was utilized to label multiple cell lines, and incorporation of azido groups was achieved on cell surfaces. The labelling activity was suppressed when the DTD activity was inhibited; this demonstrated the trigger-specific metabolic activity of HQ-NN-AAM.

To achieve controlled labeling with trigger responsiveness, two main requirements of the caging groups have to be met. First, the caged precursor should be efficiently de-caged under the designated trigger condition. Second, the cage group must resist non-specific degradation in a complex cellular environment when the trigger is absent (Fig. 1a). We synthesized four model compounds (Fig. 1b) to study suitable types of bond linkages at the anomeric position of ManNAz that could resist cleavage under complex subcellular environments. The anomeric hydroxyl position of ManNAz was caged with acetyl (Ac-AAM, ester linkage), ethoxycarbonyl (Et-O-AAM, carbonate linkage), *N*-butylcarbamate (Bu-N-AAM, carbamate linkage), and *N*-methyl-*N*-((Boc-methylamido)ethyl)carbamate (Boc-NN-AAM, *N*-methyl carbamate linkage). We incubated these four caged sugars with a panel of six different cell lines at a concentration of 50 μM for three days. The cell lines include Bxpc-3 (pancreatic cancer cells), Miapaca-2 (pancreatic cancer cells), A549 (lung cancer cells), MDA-MB-231 (breast cancer cells), HEK293 (embryonic kidney cell), and IMR90 (fibroblast cells). The azide labeling in all cells was analyzed by flow cytometry using DBCO-Cy5 as a probe. The cell surface azido glycan density was quantified through average Cy5 fluorescence intensity per cell. The labeling results (Fig. 1c) showed that the ester linkage (Ac-AAM) and the carbonate linkage (Et-O-AAM) could not block the metabolic process; this resulted in a high metabolic labeling level in all the six cell lines presumably due to the non-specific hydrolysis of the ester and the carbonate bonds by intracellular esterases.[2,25] Carbamate linkage (Bu-N-AAM), on the other hand, showed partial blocking of the labeling, with reduced Cy5 fluorescence as compared to that of Ac-AAM and Et-O-AAM at the same sugar concentration.

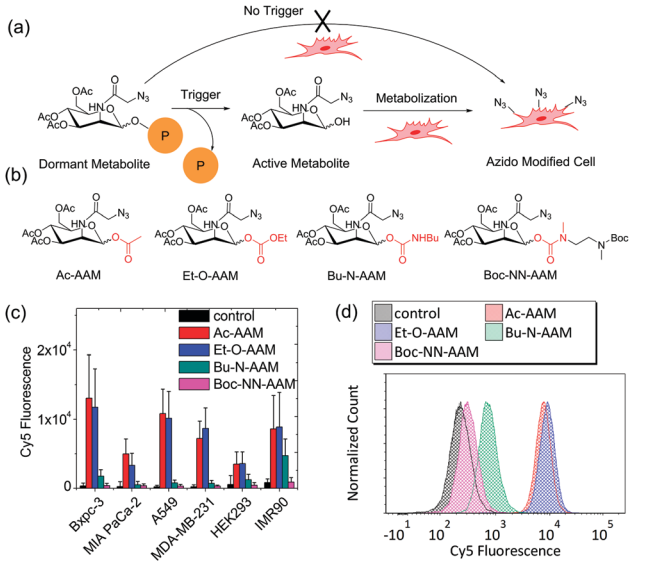

Fig. 1 Metabolic labeling of *N*-azidoacetylmannosamine is blocked by modification of the *N*-methyl carbamate linker on the 1-hydroxyl group. (a) Schematic of the controlled metabolic labeling through caging strategy. The dormant sugar activation depended solely on the cellular trigger signal. (b) Chemical structures of four control metabolic precursors with different linkers. (c) Metabolic labeling of he control metabolic precursors (50 μM) in multiple cell lines. (d) Representative flow cytometry histogram of the metabolic labeling of control precursors in MDA-MB-231 cells.

The *N*-methyl carbamate linkage (Boc-NN-AAM) showed negligible labeling in all six cell lines; this indicated the promise of the linker for blocking the metabolic process of ManNAz. As shown by the typical flow cytometry trace (Fig. 1d), the cells treated with Boc-NN-AAM showed similar fluorescence as compared to the cells without any treatment; this indicated that the signal was predominantly contributed by the passive uptake of DBCO-Cy5. On the other hand, cells treated with Ac-AAM or Et-O-AAM displayed higher fluorescence signal distribution, indicating the predominant role of the cell surface azido group attaching DBCO-Cy5 through the Click reaction.

DTD has been reported to be overexpressed in multiple cancer cell lines, and its high activity has been associated with hypoxia and cancer cell aggressiveness.[26] By incorporating a previously selected best performing *N*-methyl carbamate linker, we designed a DTD-responsive metabolic precursor, HQ-NN-AAM (Scheme 1). The conjugate consists of three major components: the HQ moiety that can be specifically reduced by DTD,[21] the NN linker with a *N*-methyl carbamate linkage that can self-cyclize when the end amine is exposed,[23] and the metabolic active precursor of triacetylated ManNAz (Fig. 2a). The synthetic route (Scheme 2) started with HQ-COOH, which was prepared according to the literature by oxidizing the lactone precursor using *N*-bromosuccinimide (NBS).[21] HQ-COOH was coupled with mono-Boc-protected *N*,*N*′-dimethylethylenediamine with *N*,*N*′-dicyclohexylcarbodiimide (DCC), *N*-hydroxysuccinimide (NHS), and 4-dimethylaminopyridine (DMAP). The Boc-protecting group was then removed in TFA/DCM. Ac_3ManNAz-OH was synthesized according to the literature report.[14] It was then activated

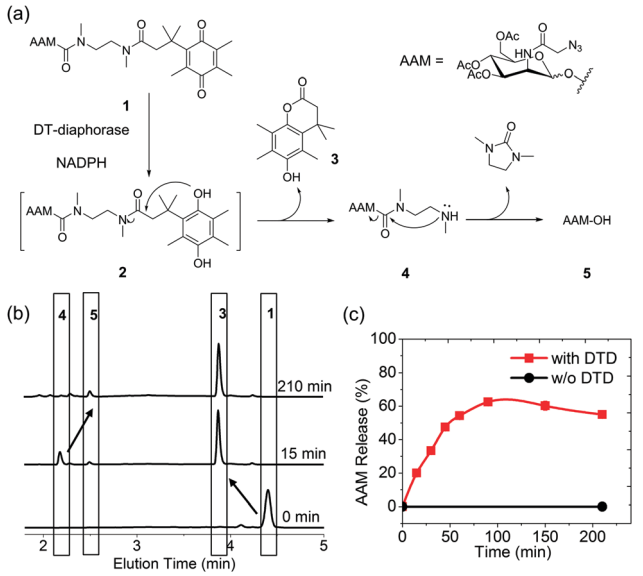

Fig. 2 DTD-responsive release of Ac_3ManNAz-OH from HQ-NN-AAM. (a) Schematic of the cascade degradation of HQ-NN-AAM under he DTD trigger. (b) HPLC trace of HQ-NN-AAM (**1**), compound **3** (15 min), compound **4** (15 min), and Ac_3ManNAz-OH (AAM-OH, 210 min). (c)' Accumulative release of Ac_3ManNAz-OH from HQ-NN-AAM with (red) or without (black) DTD. The slightly lower release of AAM was due to further hydrolysis of AAM-OH.

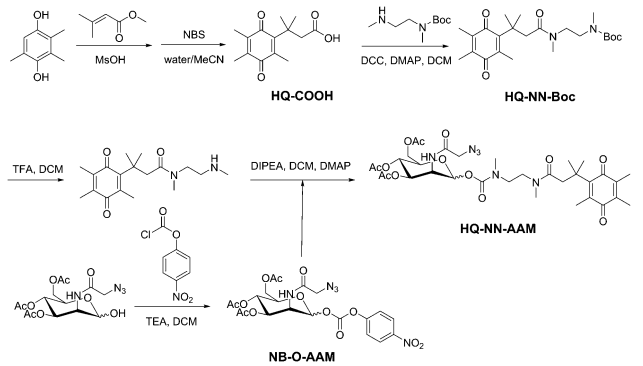

Scheme 2 Schematic of the synthesis of HQ-NN-AAM.

using 4-nitrophenyl chloroformate to NB-O-AAM and coupled with HQ-NN under mild basic conditions.

After obtaining the caged sugar, we examined the trigger-responsive decaging process under physiological conditions of HQ-NN-AAM by HPLC. The designed decaging mechanism is shown in Fig. 2a. After reduction to hydroquinone by DTD from the trimethylquinone structure, the cage group undergoes cyclization into lactone and exposes the amine group of the NN linker that also cyclizes into a five-membered cyclic urea and exposes the anomeric hydroxy group on ManNAz, finishing the decaging cascade process. We characterized this degradation process under mimicked physiological conditions (37 °C, pH = 7.4). HQ-NN-AAM was first reduced in the presence of DTD and NADPH,[27] resulting in hydroquinone **2**. The hydroquinone structure then cyclized into compounds **3** and **4** in less than 15 min. The products were characterized by LC-MS and HPLC (Fig. 2b). Compound **4** then undergoes pH-dependent cyclization (Fig. S1, ESI†) and yields the active metabolic reagent Ac_3ManNAz-OH (AAM-OH) (Fig. 2b). The accumulative release of AAM into the reaction mixture reached a plateau of 60% at around 2 h and slightly decreased afterwards presumably because of the further hydrolysis of the pendant acetyl groups with increased hydrophilicity. In comparison, NADPH was not able to trigger the decaging process of HQ-NN-AAM in the absence of DTD, and there was only negligible degradation from the hydrolysis of the pendant acetyl groups (Fig. 2c, black curve). These results indicated that HQ-NN-AAM was able to respond specifically to enzymatic degradation cues and release active metabolites efficiently within a few hours.

We examined the metabolic labeling of HQ-NN-AAM in cell lines with reportedly high DTD activity. We used MDA-MB-231[26] and Bxpc-3[28] as model cell lines. HQ-NN-AAM showed efficient labeling in cells, and the cell surface azide incorporation was confirmed by flow cytometry analysis (Fig. 3a). Boc-NN-AAM, which shares the same NN linker with the inert Boc end group, shows minimal azide labeling, whereas HQ-NN-AAM is able to efficiently label cells, evidenced by the strong DBCO-Cy5 fluorescence (Fig. 3b). The metabolic labeling of the azido sugar was also confirmed by laser scanning confocal microscopy (Fig. 3d). The Cy5 fluorescence intensity and distribution of cells incubated with the same concentrations of Boc-NN-AAM and HQ-NN-AAM showed distinct differences. The continuous red fluorescence on the cell surface (co-localization with membrane stain, Fig. S2, ESI†) resulting from HQ-NN-AAM incubation indicated successful metabolic incorporation of the azido sugar because

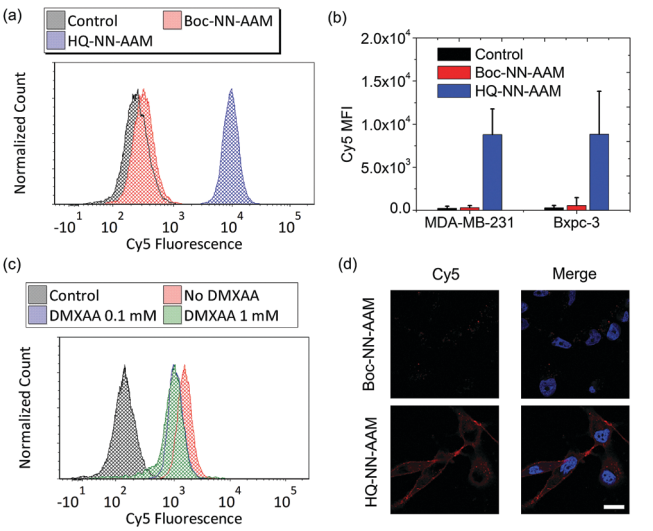

Fig. 3 HQ-NN-AAM-metabolic-labelled cells. (a) Flow cytometry histogram of metabolic labeling of HQ-NN-AAM (50 μM) and Boc-NN-AAM (50 μM) in MDA-MB-231 cells. (b) Quantification of azido labeling in MDA-MB-231 cells and Bxpc-3 cells. (c) Flow cytometry histogram of metabolic labeling of HQ-NN-AAM (50 μM) with co-incubation of the DTD inhibitor in MDA-MB-231 cells. (d) Confocal microscopy images of HQ-NN-AAM- and Boc-NN-AAM-treated MDA-MB-231 cells. The azido groups were labeled with DBCO-Cy5 (red) for visualization. The nucleus was stained with Hoechst dye (blue). Scale bar = 20 μm.

of the decaging of the HQ moiety in cells. On the other hand, cells treated with Boc-NN-AAM only showed a weak punctuated red fluorescence signal that was attributed to the background cellular uptake of DBCO-Cy5; the metabolic labeling of HQ-NN-AAM was further validated using a western blot assay (Fig. S3, ESI†). Cell surface azido concentration showed a positive correlation with the HQ-NN-AAM concentration ranging from 100 nM to 50 μM (Fig. S4, ESI†). We also performed labeling kinetic studies in MDA-MB-231 cells (Fig. S5, ESI†). HQ-NN-AAM showed labeling kinetics similar to the Ac_4ManNAz kinetics reported in the literature,[14] and an azido concentration plateau was reached at around 48 hours of incubation. This result indicated that the triggered releasing process of HQ-NN-AAM did not delay the metabolic process of ManNAz incorporated into the cell surface glycan; this was presumably due to the relatively fast release of AAM-OH from HQ-NN-AAM under physiological conditions.

We then demonstrated the specificity of HQ-NN-AAM in response to endogenous DTD using the inhibition assay. 5,6-Dimethylxanthenone-4-acetic acid (DMXAA) was used as an inhibitor of the enzymatic activity of DTD.[27] The surface azide concentration of MDA-MB-231 cells obtained upon incubation with HQ-NN-AAM reduced after pre-treatment with DMXAA (Fig. 3c), whereas the labeling of Ac_4ManNAz was not interfered by the inhibitor (Fig. S6, ESI†). The western blot assay also confirmed the reduction in the total azido sugar glycosylation level in cells treated with DMXAA (Fig. S7, ESI†). The residue metabolic labeling at high concentrations of inhibitor was presumably attributed to the non-specific reduction of the HQ moiety by other reductases in cellular environments.

In this study, we demonstrated that the *N*-methyl carbamate linker incorporated at the anomeric position of ManNAz successfully controlled the metabolic property of an unnatural sugar. The NN linker completely blocked its metabolic processes when caged and fully resumed its metabolic activity after being decaged. We synthesized HQ-NN-AAM that was reduced by DTD/NADPH and underwent a subsequent self-immolative process to yield active metabolic species. The incorporation of unnatural sugars into cell surface glycans was confirmed using HQ-NN-AAM as a labeling reagent. The *in vitro* labeling experiments demonstrated the specificity of HQ-NN-AAM that responded to DTD. This study not only demonstrates DTD-responsive metabolic labeling of the caged precursor, but also provides a deep insight into developing future metabolically active species that respond to endogenous cues in cells.

J. C. acknowledges the support received from the United States National Institute of Health Grant NIH-R21 1R21CA198684 and 1R01CA207584. R. W. was supported by the National Institute of Biomedical Imaging And Bioengineering of the National Institutes of Health under Award Number T32EB019944. The content is solely the responsibility of the authors and does not necessarily represent the official views of the National Institutes of Health.

Conflicts of interest

There are no conflicts to declare.

Notes and references

1 E. Saxon and C. R. Bertozzi, *Science*, 2000, **287**, 2007–2010.
2 J. A. Prescher, D. H. Dube and C. R. Bertozzi, *Nature*, 2004, **430**, 873–877.
3 B. Cheng, R. Xie, L. Dong and X. Chen, *ChemBioChem*, 2016, **17**, 11–27.
4 P. V. Chang, J. A. Prescher, E. M. Sletten, J. M. Baskin, I. A. Miller, N. J. Agard, A. Lo and C. R. Bertozzi, *Proc. Natl. Acad. Sci. U. S. A.*, 2010, **107**, 1821–1826.
5 J. C. Jewett and C. R. Bertozzi, *Chem. Soc. Rev.*, 2010, **39**, 1272–1279.
6 S. T. Laughlin and C. R. Bertozzi, *Nat. Protoc.*, 2007, **2**, 2930–2944.
7 R. Xie, L. Dong, R. Huang, S. Hong, R. Lei and X. Chen, *Angew. Chem., Int. Ed.*, 2014, **53**, 14082–14086.
8 M. L. Huang, S. C. Purcell, S. Verespy, Y. N. Wang and K. Godula, *Biomater. Sci.*, 2017, **5**, 1537–1540.
9 J. E. Hudak, S. M. Canham and C. R. Bertozzi, *Nat. Chem. Biol.*, 2014, **10**, 69–75.
10 E. C. Woods, N. A. Yee, J. Shen and C. R. Bertozzi, *Angew. Chem., Int. Ed.*, 2015, **54**, 15782–15788.
11 H. Koo, S. Lee, J. H. Na, S. H. Kim, S. K. Hahn, K. Choi, I. C. Kwon, S. Y. Jeong and K. Kim, *Angew. Chem., Int. Ed.*, 2012, **51**, 11836–11840.
12 S. Lee, H. Koo, J. H. Na, S. J. Han, H. S. Min, S. J. Lee, S. H. Kim, S. H. Yun, S. Y. Jeong, I. C. Kwon, K. Choi and K. Kim, *ACS Nano*, 2014, **8**, 2048–2063.
13 H. Wang, M. Gauthier, J. R. Kelly, R. J. Miller, M. Xu, W. D. O'Brien, Jr. and J. Cheng, *Angew. Chem., Int. Ed.*, 2016, **55**, 5452–5456.
14 H. Wang, R. Wang, K. Cai, H. He, Y. Liu, J. Yen, Z. Wang, M. Xu, Y. Sun, X. Zhou, Q. Yin, L. Tang, I. T. Dobrucki, L. W. Dobrucki, E. J. Chaney, S. A. Boppart, T. M. Fan, S. Lezmi, X. Chen, L. Yin and J. Cheng, *Nat. Chem. Biol.*, 2017, **13**, 415–424.
15 X. J. Wu, Y. P. Tian, M. Z. Yu, B. J. Lin, J. H. Han and S. F. Han, *Biomater. Sci.*, 2014, **2**, 1120–1127.
16 R. Xie, S. Hong, L. Feng, J. Rong and X. Chen, *J. Am. Chem. Soc.*, 2012, **134**, 9914–9917.
17 R. Xie, L. Dong, Y. Du, Y. Zhu, R. Hua, C. Zhang and X. Chen, *Proc. Natl. Acad. Sci. U. S. A.*, 2016, **113**, 5173–5178.
18 P. V. Chang, D. H. Dube, E. M. Sletten and C. R. Bertozzi, *J. Am. Chem. Soc.*, 2010, **132**, 9516–9518.
19 M. K. Shim, H. Y. Yoon, J. H. Ryu, H. Koo, S. Lee, J. H. Park, J. H. Kim, S. Lee, M. G. Pomper, I. C. Kwon and K. Kim, *Angew. Chem., Int. Ed.*, 2016, **55**, 14698–14703.
20 M. Zelzer, S. J. Todd, A. R. Hirst, T. O. McDonald and R. V. Ulijn, *Biomater. Sci.*, 2013, **1**, 11–39.
21 P. Liu, J. Xu, D. Yan, P. Zhang, F. Zeng, B. Li and S. Wu, *Chem. Commun.*, 2015, **51**, 9567–9570.
22 N. Kwon, M. K. Cho, S. J. Park, D. Kim, S. J. Nam, L. Cui, H. M. Kim and J. Yoon, *Chem. Commun.*, 2017, **53**, 525–528.
23 W. S. Saari, J. E. Schwering, P. A. Lyle, S. J. Smith and E. L. Engelhardt, *J. Med. Chem.*, 1990, **33**, 97–101.
24 A. Alouane, R. Labruere, T. Le Saux, F. Schmidt and L. Jullien, *Angew. Chem., Int. Ed.*, 2015, **54**, 7492–7509.
25 A. D. Quiroga and R. Lehner, *Trends Endocrinol. Metab.*, 2011, **22**, 218–225.
26 Y. Yang, Y. Zhang, Q. Wu, X. Cui, Z. Lin, S. Liu and L. Chen, *J. Exp. Clin. Cancer Res.*, 2014, **33**, 14–22.
27 R. M. Phillips, *Biochem. Pharmacol.*, 1999, **58**, 303–310.
28 M. Ji, A. Jin, J. Sun, X. Cui, Y. Yang, L. Chen and Z. Lin, *Oncol. Lett.*, 2017, **13**, 2996–3002.